Coupling AAV-mediated promoterless gene targeting to SaCas9 nuclease to efficiently correct liver metabolic diseases

Alessia De Caneva[1], Fabiola Porro[1], Giulia Bortolussi[1], Riccardo Sola[1], Michela Lisjak[1], Adi Barzel[2], Mauro Giacca[1], Mark A. Kay[3], Kristian Vlahovicek[4], Lorena Zentilin[1] and Andrés F. Muro[1*]

Supplementary Materials

Supplementary Figures

Supplementary Tables

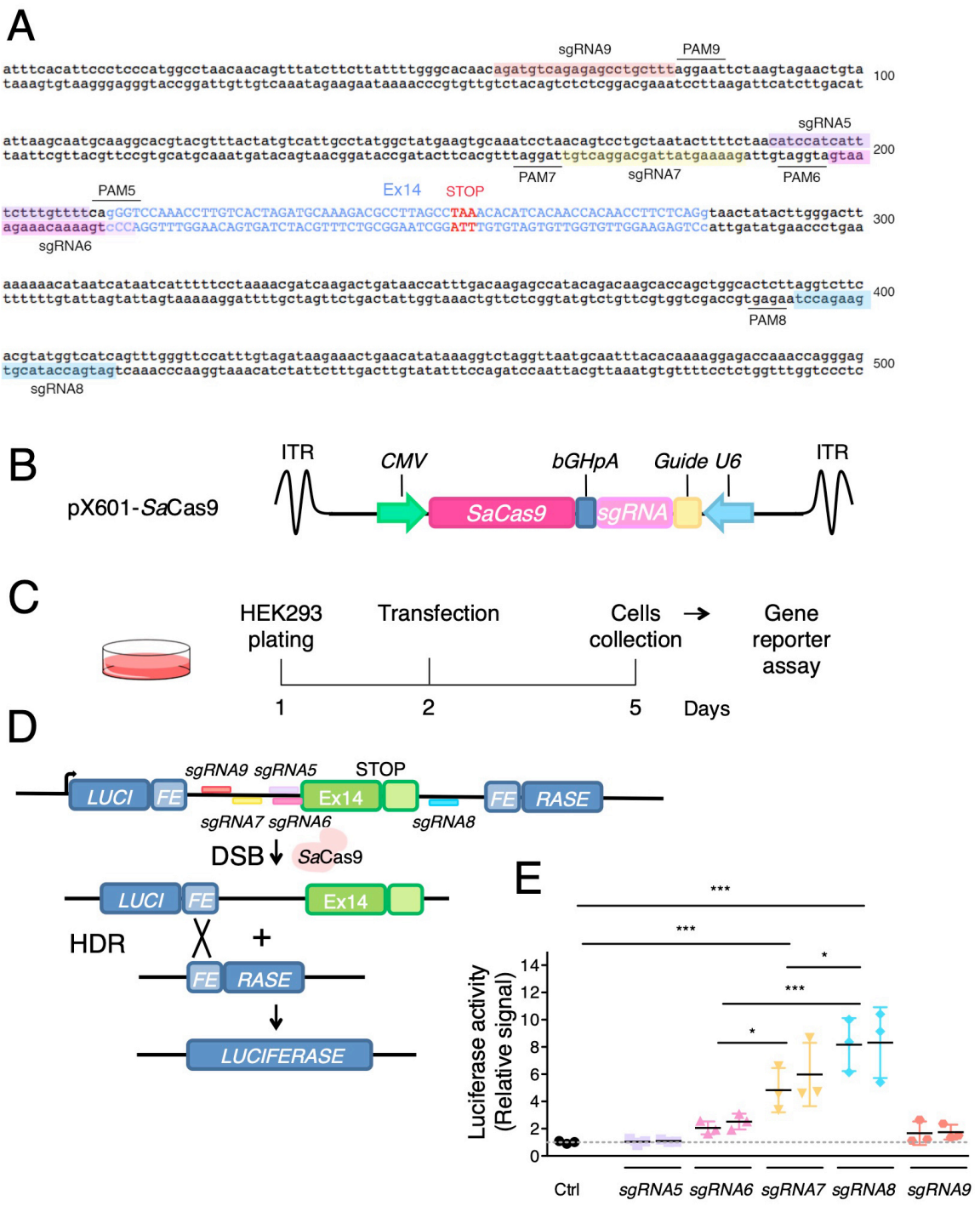

Figure S1. Design of sgRNAs and in vitro testing with a reporter vector. (**A**) The albumin exon 14 (capital letters), stop codon (STOP), flanking introns (small caps), and the identified sgRNAs are shown. (**B**) Scheme of the pX601-*Sa*Cas9 vector. ITR, inverted terminal repeat; CMV, Cytomegalovirus promoter; *Sa*Cas9, *Staphylococcus aureus* Cas9; bGHpA, bovine growth hormone polyadenylation signal; sgRNA, single guide RNA; Guide, incomplete sgRNA-coding sequence; U6, RNA polIII promoter. (**C**) Scheme of the experimental design. HEK293 cells were transiently transfected with the pX601-*Sa*Cas9 plasmid and the homologous recombination reporter vector, and luciferase activity was determined. (**D**) Scheme of the homologous recombination reporter vector and resulting recombination product. The recombination reporter vector (34) contained the albumin exon 14 and flanking introns. Recombination between the repeated luciferase sequences results in the reconstitution of luciferase activity. (**E**) The dot plot graph shows the luciferase activity determined after transfection of the pX601-*Sa*Cas9 vectors (low and a high amounts). Values are normalized respect to cells transfected with the reporter vector alone (Ctrl). Two-way ANOVA: interaction, ns, $P = 0.9569$; sgRNA, ***, $P < 0.0001$; dose, ns, $P = 0.4743$; Bonferroni *post hoc* tests analysis; experiments were conducted in triplicate.

A

	Clones	Insertions	Deletions	% INDELs
sgRNA7	24	3	6	38%
sgRNA8	24	6	11	71%

B

```
mAlb          ACTATGTCATTGCCTATGGCTATGAAGTGCAAATCCTAACAGTCCTGCTAATACTTTTCTAACATCCATCATTTCTTT
cl2 Δ43       ACTATGTCATTGCCTATG------------------------------------------ACATCCATCATTTCTTT
cl4 Δ45       ACTATGTCATTGCCTA-------------------------------------------ACATCCATCATTTCTTT
cl15 Δ2       ACTATGTCATTGCCTATGGCTATGAAGTGCAAATCCTAA--GTCCTGCTAATACTTTTCTAACATCCATCATTTCTTT
cl25 Δ9       ACTATGTCATTGCCTATGGCTATGAAGTGCAAATCCT---------GCTAATACTTTTCTAACATCCATCATTTCTTT
cl26 Δ2       ACTATGTCATTGCCTATGGCTATGAAGTGCAAATCCTAA--GTCCTGCTAATACTTTTCTAACATCCATCATTTCTTT
cl27 Δ2       ACTATGTCATTGCCTATGGCTATGAAGTGCAAATCCTAA--GTCCTGCTAATACTTTTCTAACATCCATCATTTCTTT

mAlb          ACTATGTCATTGCCTATGGCTATGAAGTGCAAATCCTAACAG--------------------TCCTGCTAATACTTTTCTAACATCCATCATTTCTTT
cl3 +201      ACTATGTCATTGCCTATGGCTATGAAGTGCAAATCCTATTTT--------------------TCCTGCTAATACTTTTCTAACATCCATCATTTCTTT
cl14 +2       ACTATGTCATTGCCTATGGCTATGAAGTGCAAATCCTAACAG--------------------TCCTGCTAATACTTTTCTAACATCCATCATTTCTTT
cl16 +1       ACTATGTCATTGCCTATGGCTATGAAGTGCAAATCCTAACAA--------------------TCCTGCTAATACTTTTCTAACATCCATCATTTCTTT
```

C

```
mALB          TACAGACAAGCACCAGCTGGCACTCTTAGGTCTTCACGTATGGTCATCAGTTTGGGTTCCATTTGTAGATAAGAAAC
cl34 Δ18      TACAGACAAGCACCAGCTGGCACTCTT-----------------TTCAGTTTGGGTTCCATTTGTAGATAAGAAAC
cl35 Δ437     ------------------------------------------------------------------------------
cl40 Δ7       TACAGACAAGCACCAGCTGGCACTCT-------TCACGTATGGTCATCAGTTTGGGTTCCATTTGTAGATAAGAAAC
cl43 Δ21      TACAGACAAGCACCATACG--------------------TGGTCATCAGTTTGGGTTCCATTTGTAGATAAGAAAC
cl44 Δ2       TACAGACAAGCACCAGCTGGCACTCTTAGG--TTCACGTATGGTCATCAGTTTGGGTTCCATTTGTAGATAAGAAAC
cl46 Δ14      TACAGACAAGCACCAGCTGG--------------CACGTATGGTCATCAGTTTGGGTTCCATTTGTAGATAAGAAAC
cl48 Δ2       TACAGACAAGCACCAGCTGGCACTCTTA--TCTTCACGTATGGTCATCAGTTTGGGTTCCATTTGTAGATAAGAAAC
cl55 Δ1       TACAGACAAGCACCAGCTGGCACTCTTAG-TCTTCACGTATGGTCATCAGTTTGGGTTCCATTTGTAGATAAGAAAC
cl57 Δ2       TACAGACAAGCACCAGCTGGCACTCTTA--TCTTCACGTATGGTCATCAGTTTGGGTTCCATTTGTAGATAAGAAAC
cl58 Δ2       TACAGACAAGCACCAGCTGGCACTCTTA--TCTTCACGTATGGTCATCAGTTTGGGTTCCATTTGTAGATAAGAAAC
cl59 Δ14      TACAGACAAGCACCAG--------------TCTTCACGTATGGTCATCAGTTTGGGTTCCATTTGTAGATAAGAAAC

mALB          TACAGACAAGCACCAGCTGGCACTCTTAGG------------------TCTTCACGTATGGTCATCAGTTTGGGTTCCATTTGTAGATAA
cl31 +44      TACAGACAAGCACCAGCTGGCACTCTTAGG------------------TCTTCACGTATGGTCATCAGTTTGGGTTCCATTTGTAGATAA
cl36 +166     TACAGACAAGCACCAGCTGGCACTCTTAGG------------------TCTTCACGTATGGTCATCAGTTTGGGTTCCATTTGTAGACAA
cl41 +500     TACAGACAAGCACCAGCTGGCACTCTTAGG------------------TCTTCACGTATGGTCATCAGTTTGGGTTCCATTTGTAGATAA
cl47 +209     TACAGACAAGCACCAGCTGGCACTCTTA--------------------TCTTCACGTATGGTCATCAGTTTGGGTTCCATTTGTAGATAA
cl51 +136     TACAGACAAGCACCAGCTGGCACTCTTAGG--------------------TTCACGTATGGTCATCAGTTTGGGTTCCATTTGTAGATAA
cl56 +340     TACAGACAAGCACCAGCTGGCACTCT----------------------TCTTCACGTATGGTCATCAGTTTGGGTTCCATTTGTAGATAA
```

Figure S2. *sgRNA*8 is more efficient than *sgRNA7* to induce INDELs at the endogenous albumin locus in NIH-3T3 cells. (**A)** The PCR products obtained in Figure 2B were cloned and 24 independent clones from each sgRNA treatment were sequenced. The number of clones presenting insertions and deletions, and the total % of INDELs are indicated. (**B, C**) Alignments of the sequences of the analyzed clones treated with *Sa*Cas9-sgRNA7 (B), or *Sa*Cas9-sgRNA8 (C). Sequences were aligned to that of the mouse albumin gene (mAlb). The *sgRNA7* sequence is highlighted in yellow while the *sgRNA8* one in light blue. The corresponding PAM regions are typed in blue, while base modifications are indicated in red. The length of deletions and insertions (in bp) are indicated as Δ and +, respectively, next to the clone number (cl).

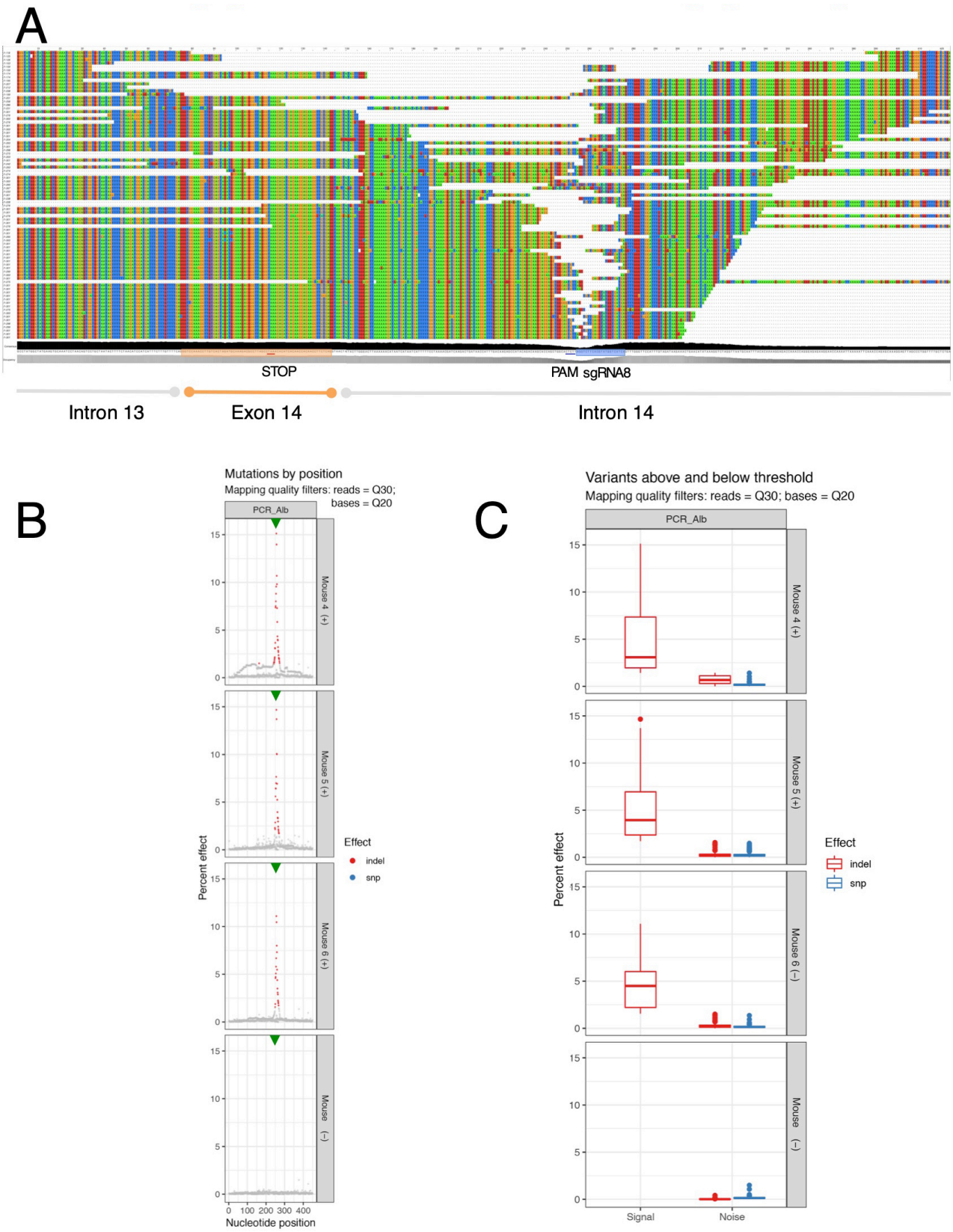

Figure S3. sgRNA8 efficiently targets the albumin locus in neonatal treated mice. (**A**) Representative nucleotide sequences of the targeted albumin locus of *sgRNA8* treated mice. Sequences shown represent gap length diversity rather than the actual frequency distribution. The length of the PCR fragment was 517 bp (**B**) Mutation frequency analysis at the albumin target site by *sgRNA8*. The dots represent the percentage of reads with bases different from the original sequence at each base position. The colored dots indicate variants above noise levels; the grey dots represent levels predicted as sequencing noise. The *Sa*Cas9 on-target site is indicated by green arrowheads. The analysis was performed in the same animals analyzed in Figure 2C-D. **(C)** Box plots of the distributions of the data shown in Panel B, with indicated median values. Signal and noise distributions are plotted separately. Indels are represented in red and snp in blue.

Vg/mouse	2.5E+11	5.0E+11	7.5E+11	1.0E+12
INDELs (%)	6.2	4.5	25.2	27.9

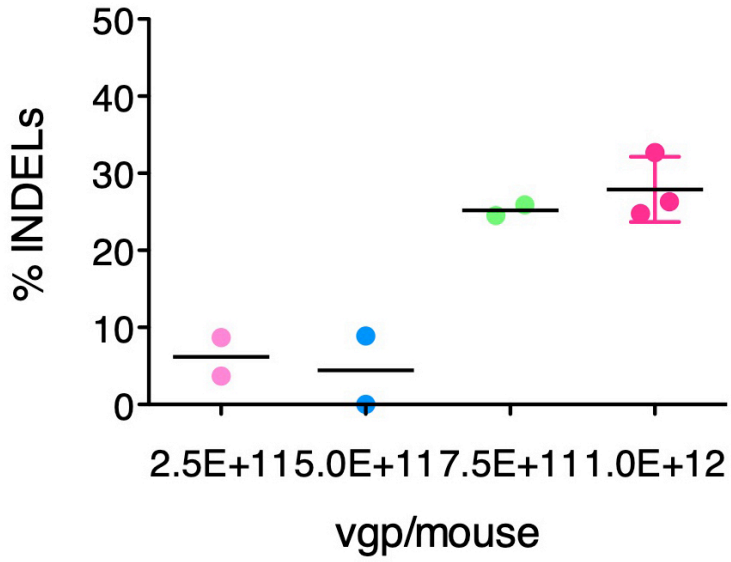

Figure S4. Determination of the most effective dose of rAAV8-*Sa*Cas9-sgRNA8. The % of INDELs obtained after transducing P4 WT pups by intraperitoneal injection are indicated. The doses used in each experimental group (n=2 mice/dose, except in the 1.0E12 group, n=3) are indicated.

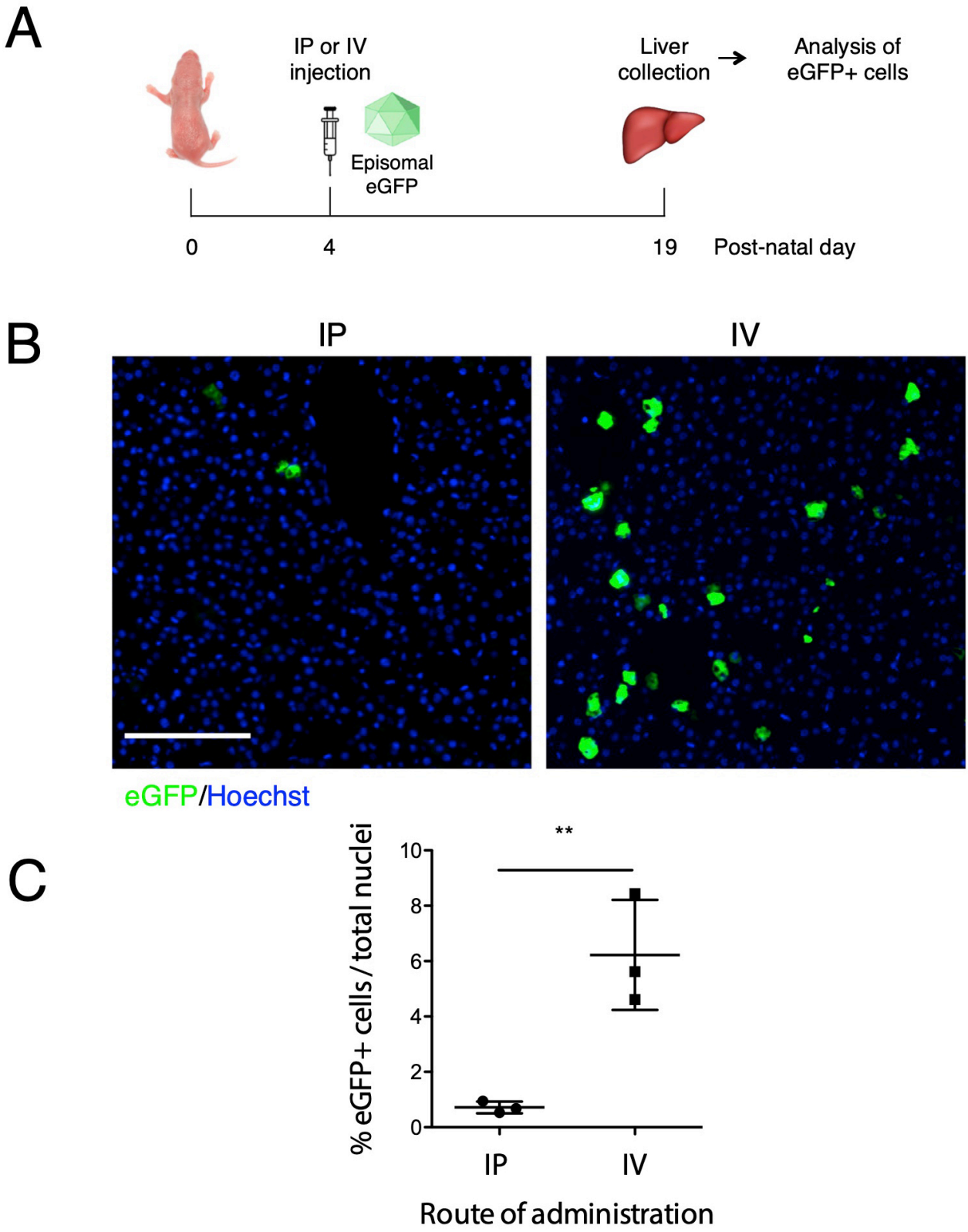

Figure S5. The intravenous route of administration is more efficient than the intraperitoneal one. (**A**) Scheme of the experimental strategy used to compare intraperitoneal (IP) and intravenous (IV) administration routes. WT newborn mice were IP or IV transduced at post-natal day 4 with the same dose (1.0E+11 vg/mouse) of the rAAV8-pGG2-AAT-*eGFP* episomal vector (13). The liver was collected at post-natal day 19 and the number of eGFP positive cells in liver sections was evaluated. (**B**) Histological analysis of liver sections of IP- or IV-transduced mice. Nuclei were counterstained with Hoechst. Representative images are shown. Scale bar 500 µm. (**C**) Quantification of the number of eGFP-positive hepatocytes. Unpaired Student's t-test, **, P = 0.0088, n = 3 per experimental group, 10 images per animal were analyzed.

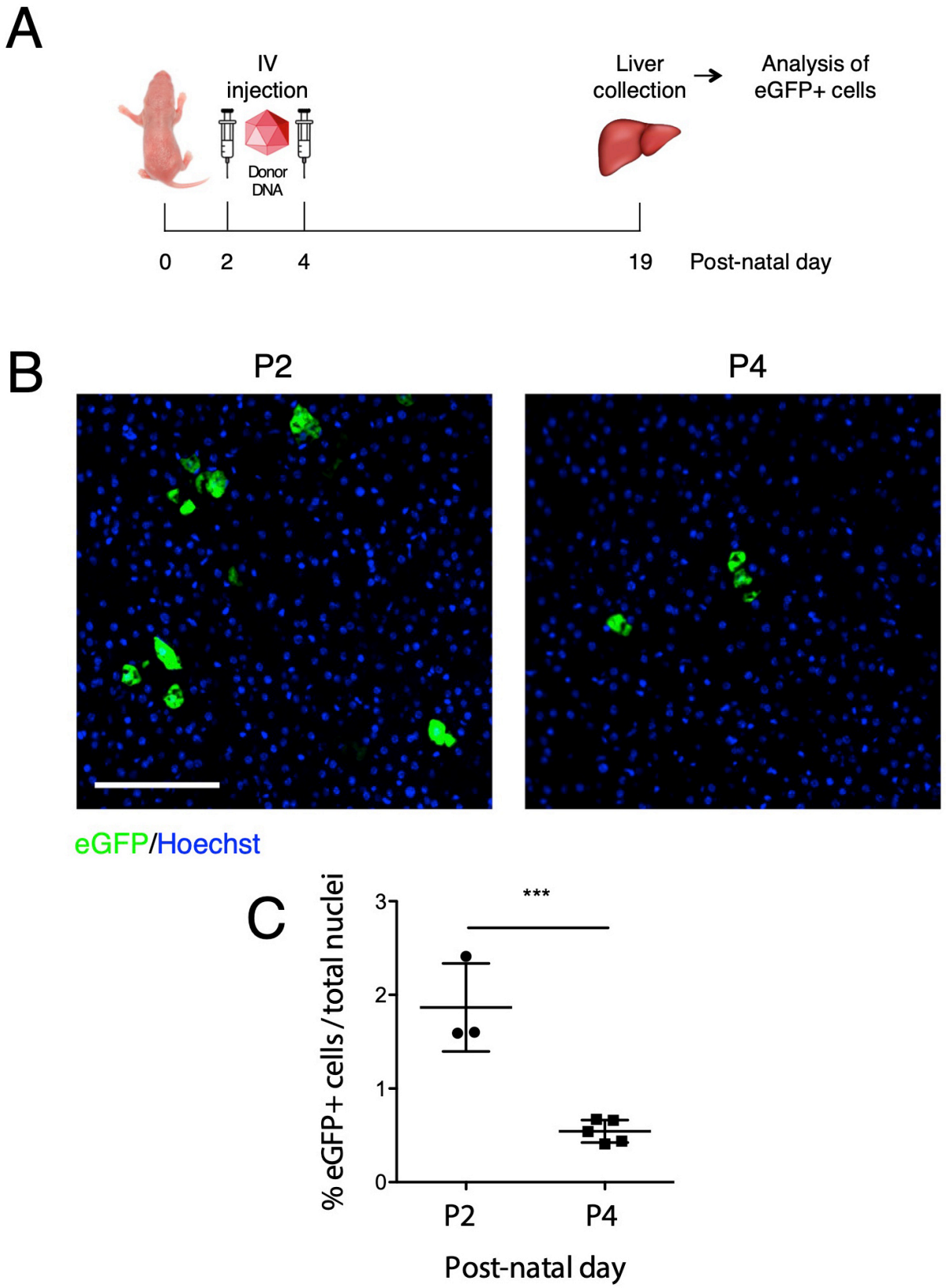

Figure S6. Spontaneous HR is more efficient at P2 administration than at P4 one. (**A**) Scheme of the experimental design. WT newborn mice were IV transduced with rAAV8-donor-*eGFP* at P2 or P4 with 8.0E11 vg/mouse of rAAV8-donor-*eGFP*. Liver was collected at P19 and the number of eGFP-positive cells was determined. (**B**) Histological analysis of liver sections. Nuclei were counterstained with Hoechst. Scale bar 500 μm. (**C**) Quantification of the number of eGFP positive hepatocytes. Unpaired Student's t-test, ***, P = 0.0008. n=3 and 5 for the animals transduced at P2 and P4, respectively; 10 images per animal were analyzed.

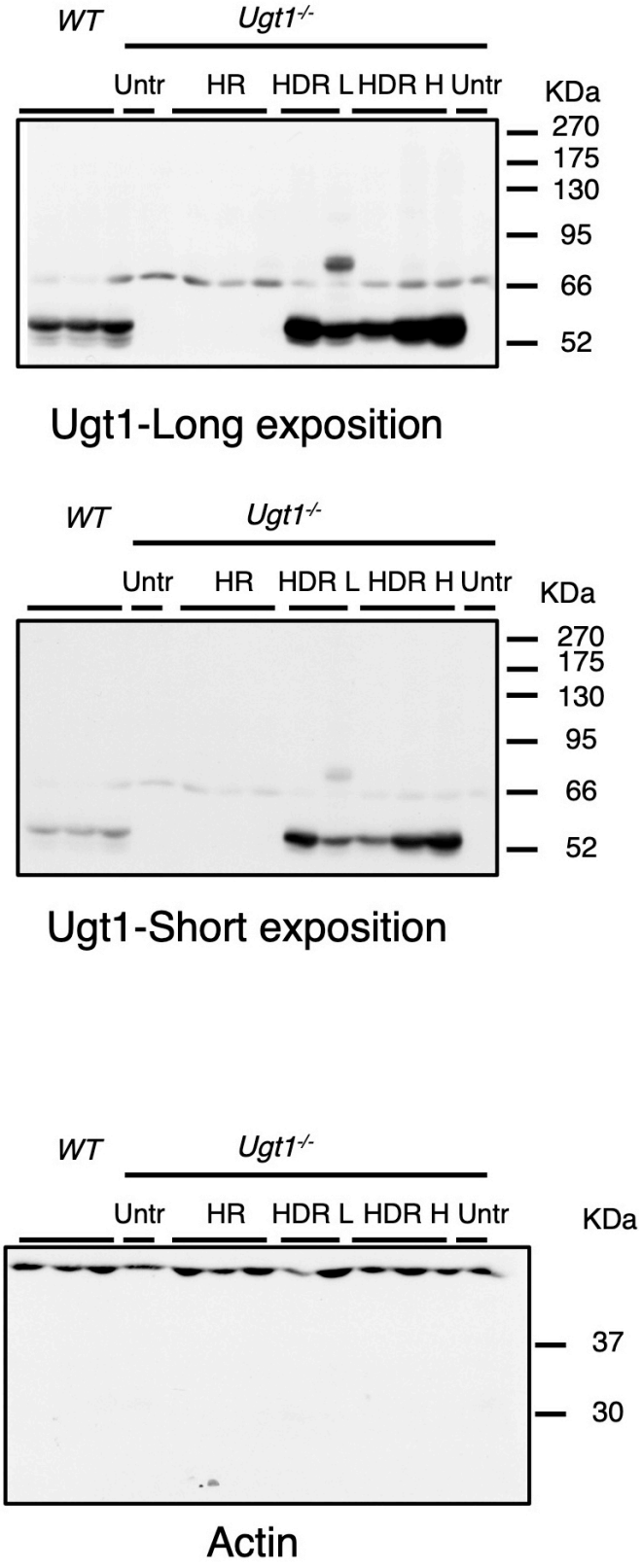

Figure S7. WB analysis of liver extracts from Crigler-Najjar mice treated with rAAV8-donor-*hUGT1A1* and rAAV8-*Sa*Cas9-sgRNA8. *Ugt1*$^{-/-}$ newborn mice were IV transduced at P2 with rAAV8-donor-*hUGT1A1* alone (HR; 2.0E11 vg/mouse) or in combination with rAAV8-*Sa*Cas9-sgRNA8, using two different *Sa*Cas9 doses (low, HDR L; or high, HDR H; 6.0E10 and 2.0E11 vg/mouse, respectively), as described in Figure 4. The complete gels of the Western blot analyses of liver protein extracts using an anti-Ugt1 antibody with human and mouse specificity are shown (Short and long expositions). No bands corresponding to the potential full length Albumin-P2A-hUGT1A1 protein were detected, suggesting efficient ribosomal skipping by the P2A.

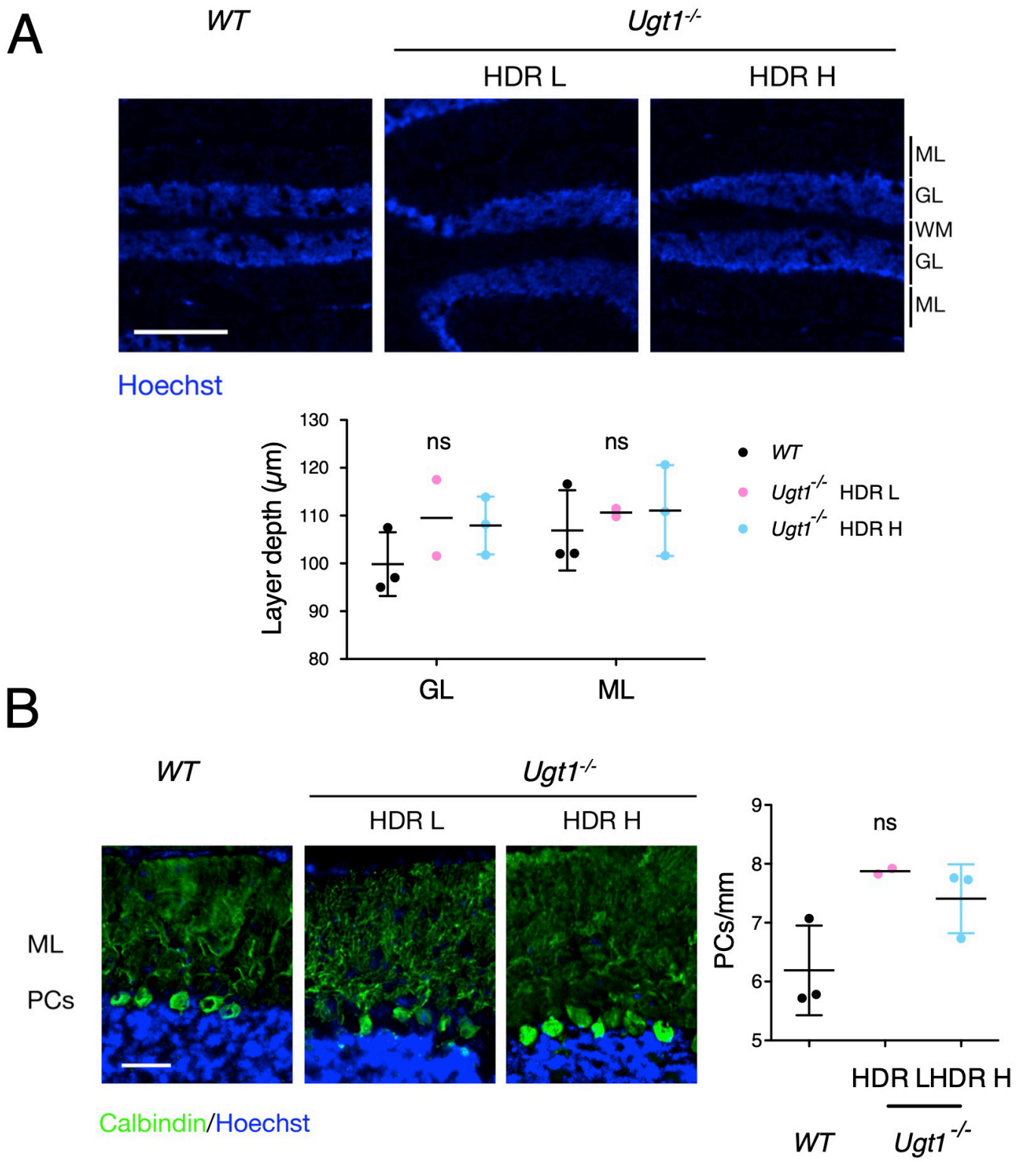

Figure S8 *Ugt1*$^{-/-}$ rAVV8-treated mice show normal brain histology. (**A**) Cerebellar layer thickness was determined in WT untreated and *Ugt1*$^{-/-}$ rAAV8-treated mice (M10) with a constant dose of the donor vector and two different *Sa*Cas9 doses (low, HDR L; or high, HDR H), using Hoechst-stained brain sections. Representative images are shown. ML, molecular layer; GL, granular layer; WM, white matter. Scale bar = 480 μm. *WT* vs. HDR H, unpaired t-test, GL: ns, P = 0.1945;. ML: ns, P= 0.6024. WT and HDR H, n = 3; HDR L, n = 2. (**B**) Left panel, Purkinje cells immunofluorescence analysis of cerebellar sections using an anti-Calbindin specific antibody. Nuclei were counterstained with Hoechst. Scale bar 50 μm. WT and HDR H, n = 3; HDR L, n = 2. ML, molecular layer; PCs, Purkinje cells. Right panel, quantification of PCs density. Student t-test, ns, P = 0.0936. The analysis was performed in the same animals used in Figure 4.

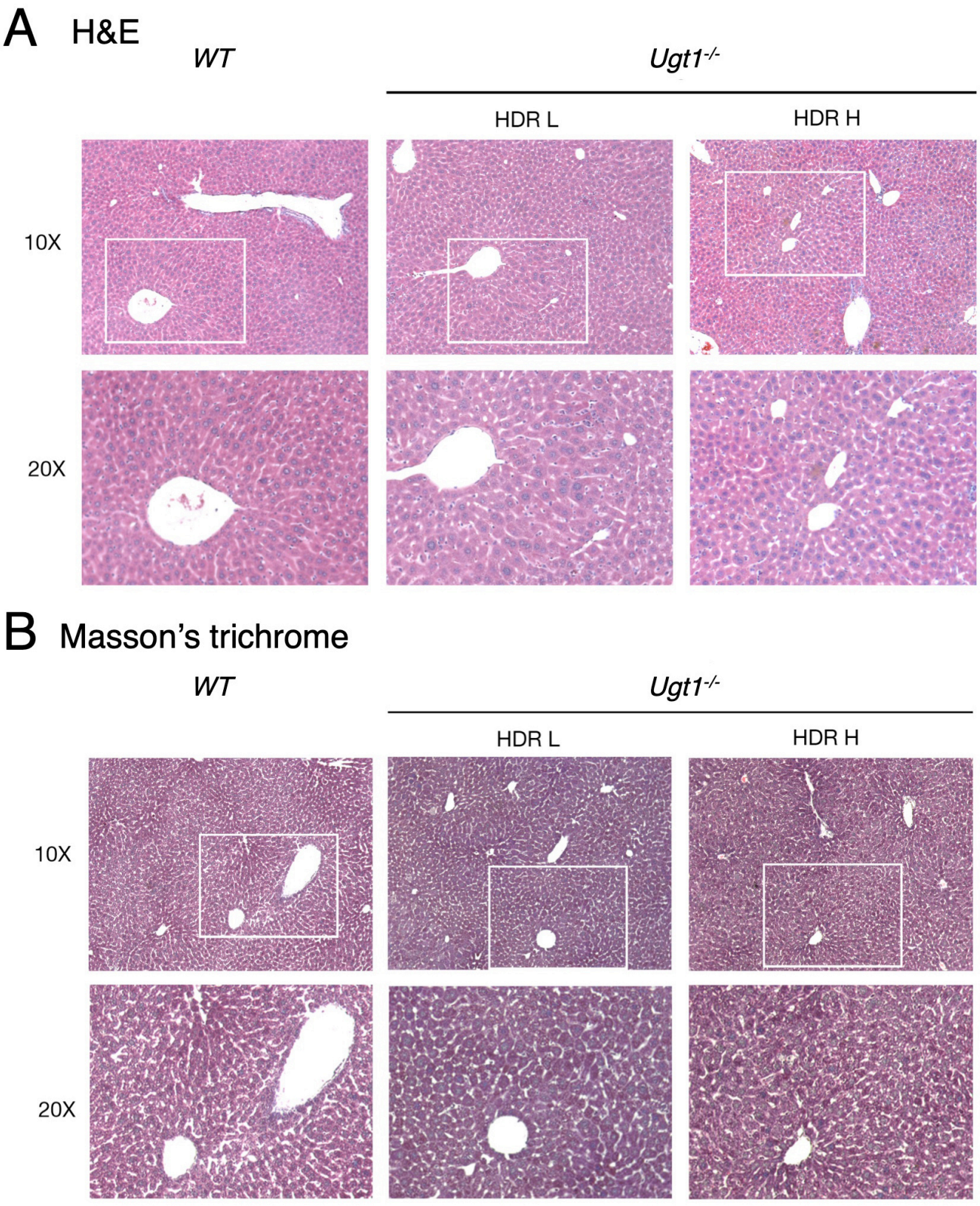

Figure S9 *Ugt1*$^{-/-}$ rAVV8-treated mice show normal liver histology. (**A**) (**B**) Haematoxylin-Eosin (H&E) (A) and Masson's trichrome (B) stainings of liver sections from WT/HET untreated and *Ugt1*$^{-/-}$ rAAV8-treated mice (M10) with a constant dose of the donor vector and two different *Sa*Cas9 doses (low, HDR L; or high, HDR H). 10 x and 20 x magnifications are shown. WT and HDR H, n = 3; HDR L, n = 2. The analysis was performed in the same animals used in Figure 4.

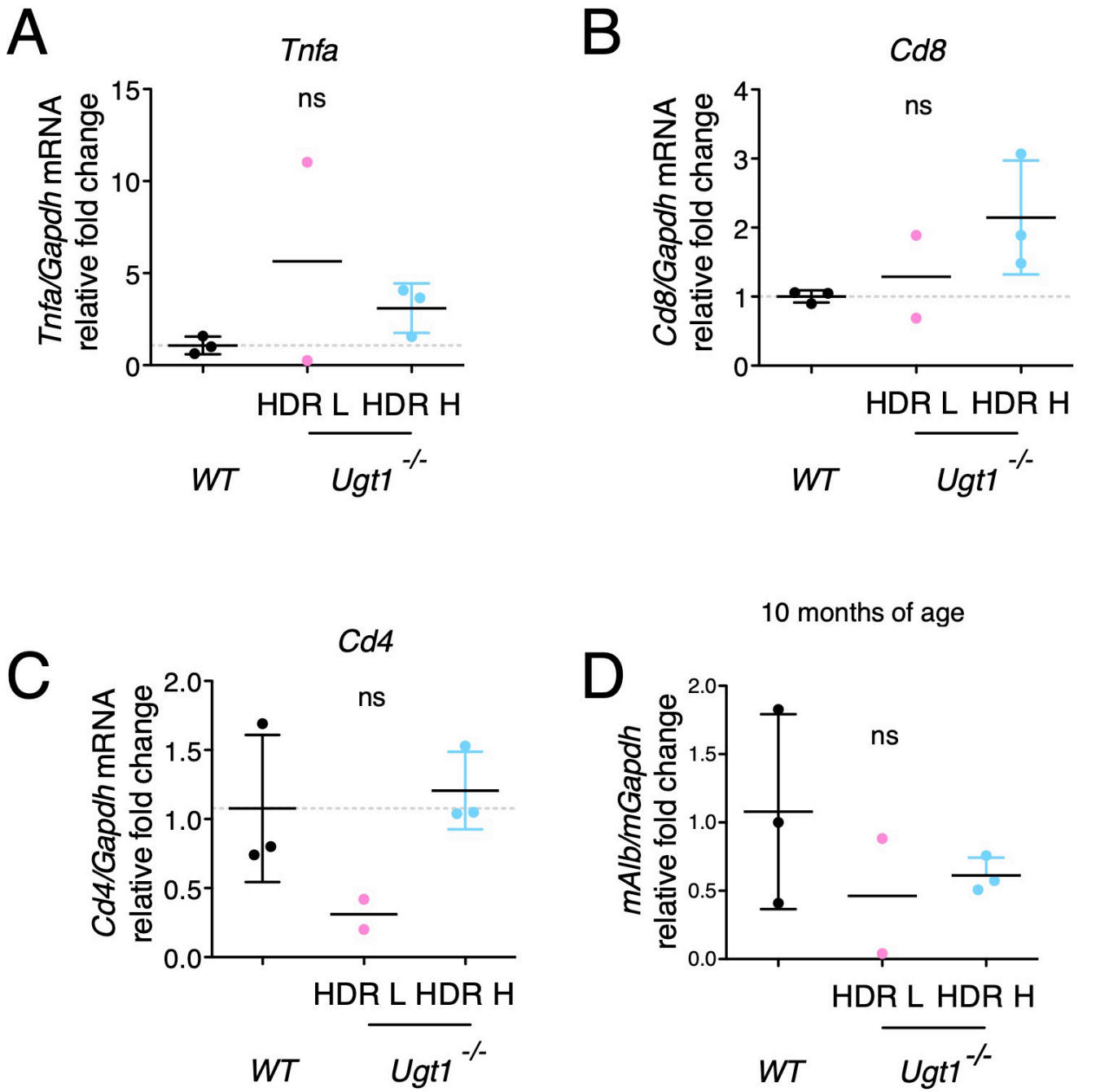

Figure S10 *Ugt1*$^{-/-}$ rAVV8-treated mice show no evidence of inflammation. (**A-D**) Evaluation of the mRNA levels by qRT-PCR of *Tnfa* (A), *Cd8* (B), *Cd4* (C) and *Infg* (D) of WT untreated and *Ugt1*$^{-/-}$ rAAV8-treated mice with two different donor-*Sa*Cas9 ratios (low, HDR L; or high, HDR H), at 10 months of age. *Gapdh* was used to normalize all inflammatory markers levels. Student t-test: *Tnfa*, ns, P = 0.0702; *Cd8*, ns, P = 0.0756; *Cd4*, ns, P = 0.7270; *Infg*, ns, P = 0.8456. HDR L, n = 2; WT and HDR H, n = 3. The analysis was performed in the same animals used in Figure 4.

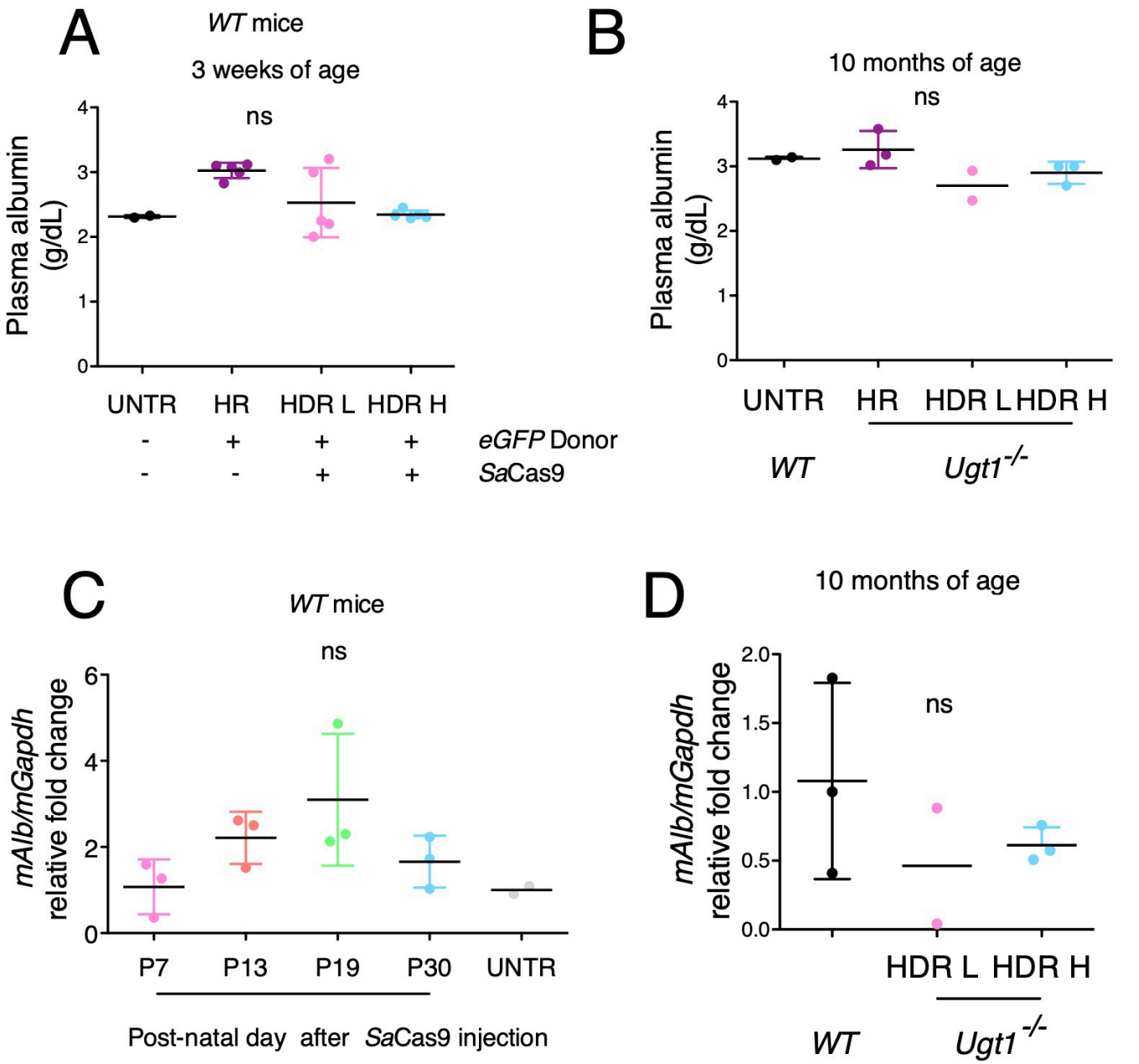

Figure S11. Normal mRNA and protein levels of albumin after *Sa*Cas9 administration. (**A**) Plasma albumin evaluation of WT mice untreated and treated at P2 with *eGFP*-donor DNA (HR), or with *eGFP*-donor DNA and *Sa*Cas9 encoding AAV8 vectors, at low (HDR L) or high *Sa*Cas9 dose (HDR H). n = 5 The analysis was performed in the same animals used in Figure 3. One-way ANOVA, ns., n = 5 per experimental group. (**B**) Plasma albumin evaluation of *WT* mice untreated and treated at P2 with a constant dose of *hUGT1A1*-donor DNA AAV, and two doses of *Sa*Cas9 encoding AAV8 vector (low, HDR L; or high, HDR H). The analysis was performed in the same animals used in Figure 4. One-way ANOVA, ns., P=0.1435, *WT* and HDR H, n=3; HDR L, n = 2. (**C**) Albumin mRNA levels of *WT* mice untreated (UNTR) and treated with only rAAV8-*Sa*Cas9-sgRNA8 (2.0E+11 vg/mouse) at P2. Mice were sacrificed at different post-natal days, (P7, P13, P19, and P30) and the livers analyzed. One-way ANOVA, ns, P = 0.5473, untreated mice, n = 2; treated mice, n = 3 per group. (**D**) Albumin mRNA levels of WT mice untreated (UNTR) and *Ugt1*$^{-/-}$ rAAV8-treated mice with a low (HDR L) and a higher ratio (HDR H) between *hUGT1A1*-donor and *Sa*Cas9 at 10 months of age. The analysis was performed in the same animals used in Figure 4. One-way ANOVA, ns, P = 0.4394; *WT* and HDR H, n=3; HDR L, n = 2.

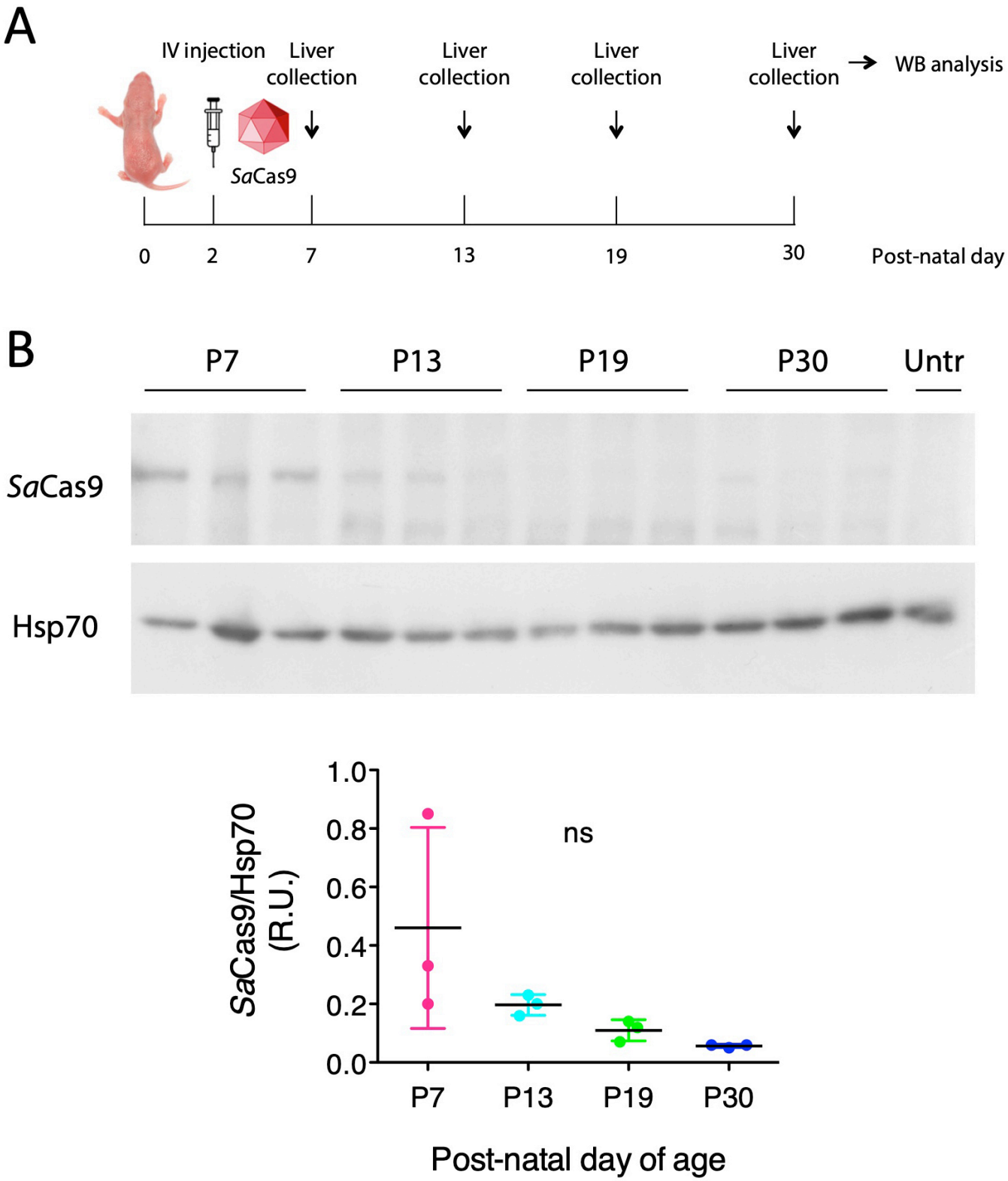

Figure S12 *Sa*Cas9 protein levels decrease to undetectable levels 30 days after its administration. (**A**) Experimental scheme. WT newborn mice were intravenously transduced with rAAV8-*Sa*Cas9-sgRNA8 (2.0E+11 vg/mouse) at post-natal day 2. Livers were collected at post-natal days 7, 13, 19 and 30, and analyzed by WB. IV, intravenous; *Sa*Cas9, rAAV8-*Sa*Cas9-sgRNA8. (**B**) WB analysis of liver protein extracts of WT untreated and treated with rAAV8-*Sa*Cas9-sgRNA8 collected at different post-natal days. HSP70 was used as loading control. The quantification of the WB is shown in the lower panel. One-way ANOVA, ns, P = 0.0847, n = 3 per group.

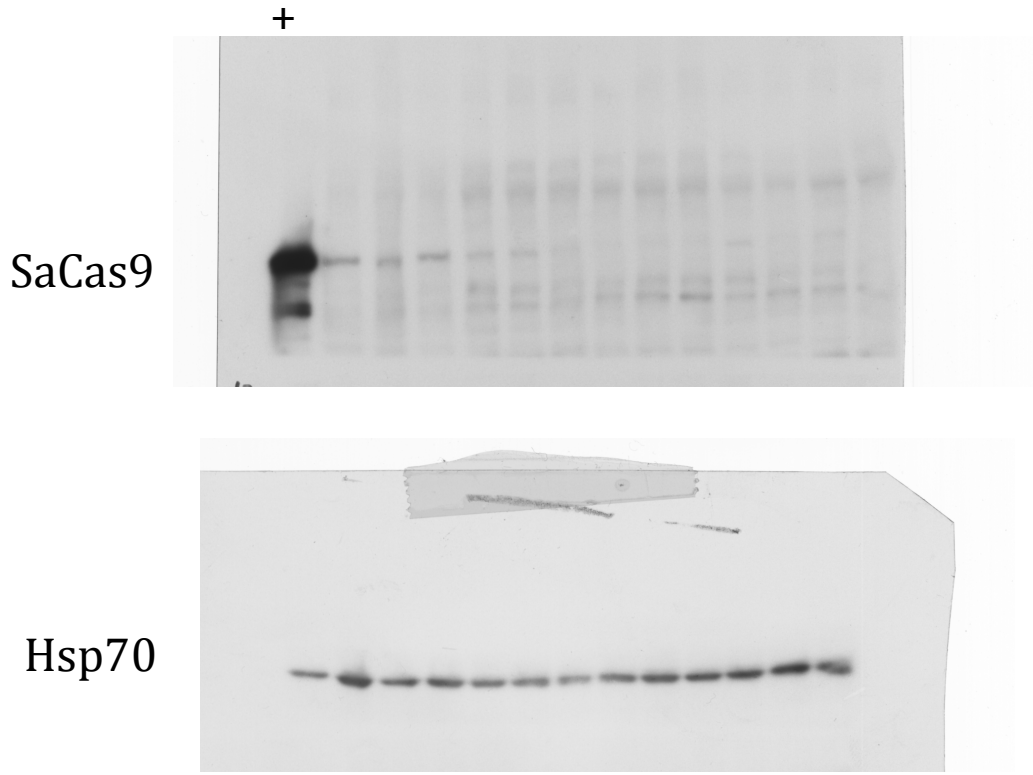

Figure S13. Full uncut gels of Figure S12. The "+" symbol in the first lane on the left indicates the positive control corresponding to tissue culture cells transfected with a plasmid expressing the SaCas9.

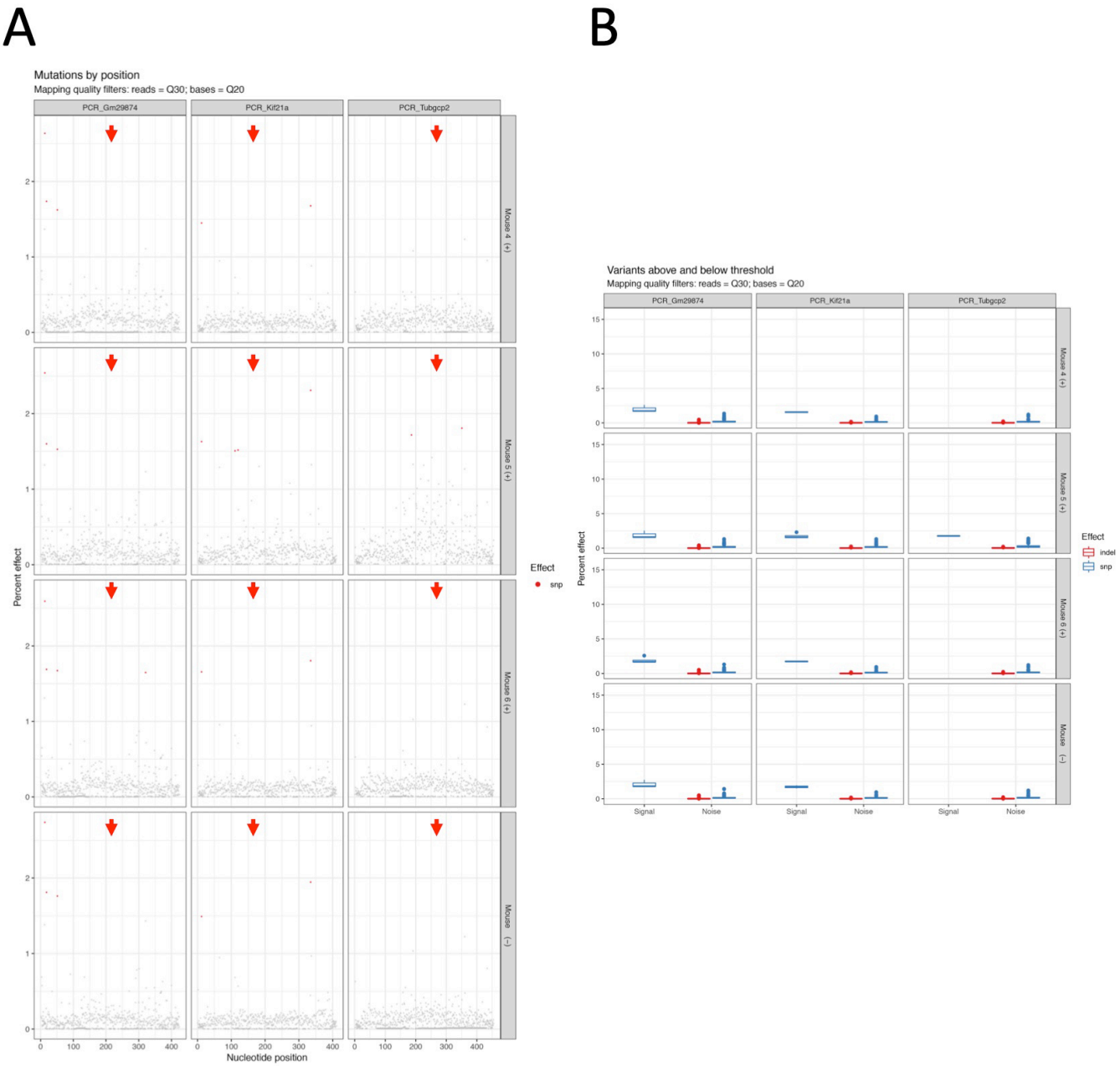

Figure S14 Analysis of *Sa*Cas9 off-target activity. (**A**). Mutation frequency analysis of the predicted potential off-target sites by *sgRNA8*. The dots represent the percentage of reads with bases different from the original sequence at each base position. The red and blue dots indicate variants above noise levels. Grey dots indicate variants below threshold levels (noise). The location of the predicted SaCas9 off-target site is indicated by a red arrow. (**B**) Box plots of the distributions of the data shown in Panel A, with indicated median values. Signal and noise distributions are plotted separately. Indels are represented in red and snp in blue. The analysis was performed in the same animals used in Figure 2C, D and Figure S3. The length of the PCR fragments was *Tubgcp*2, 522 bp; *Kif21a*, 478 bp; and *Gm29874*, 491 bp.

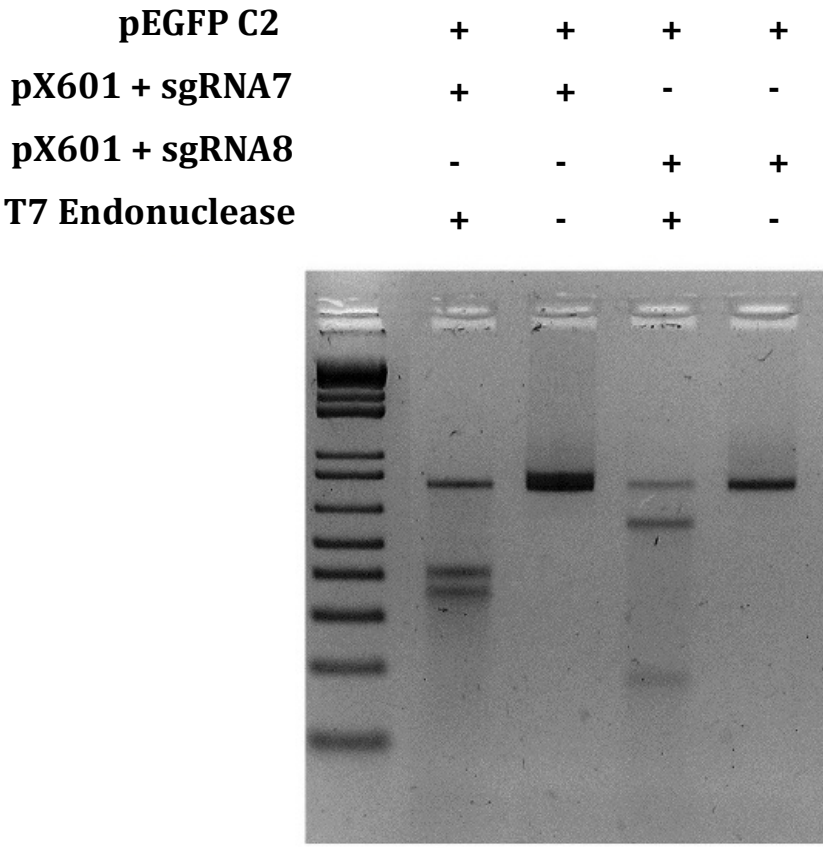

Figure S15. Full uncut gels of Figure 2B.

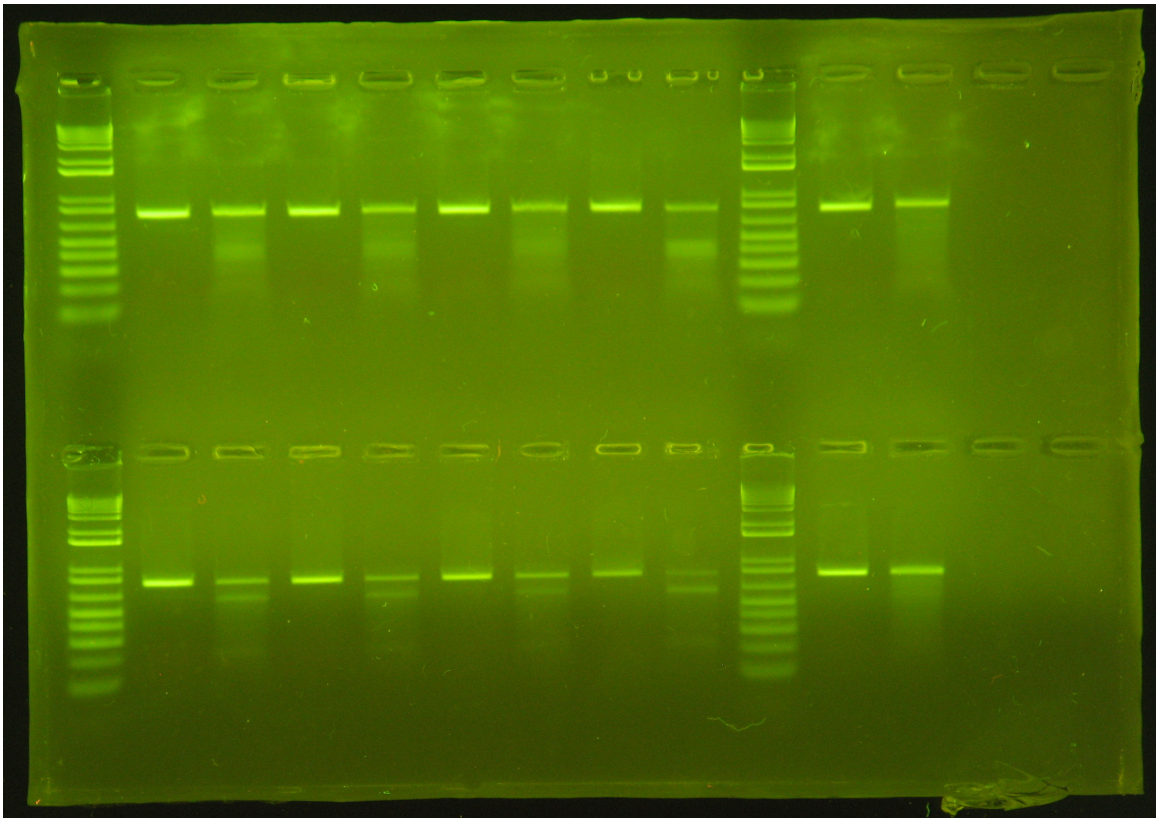

Figure S16. Full uncut gels of Figure 2D.

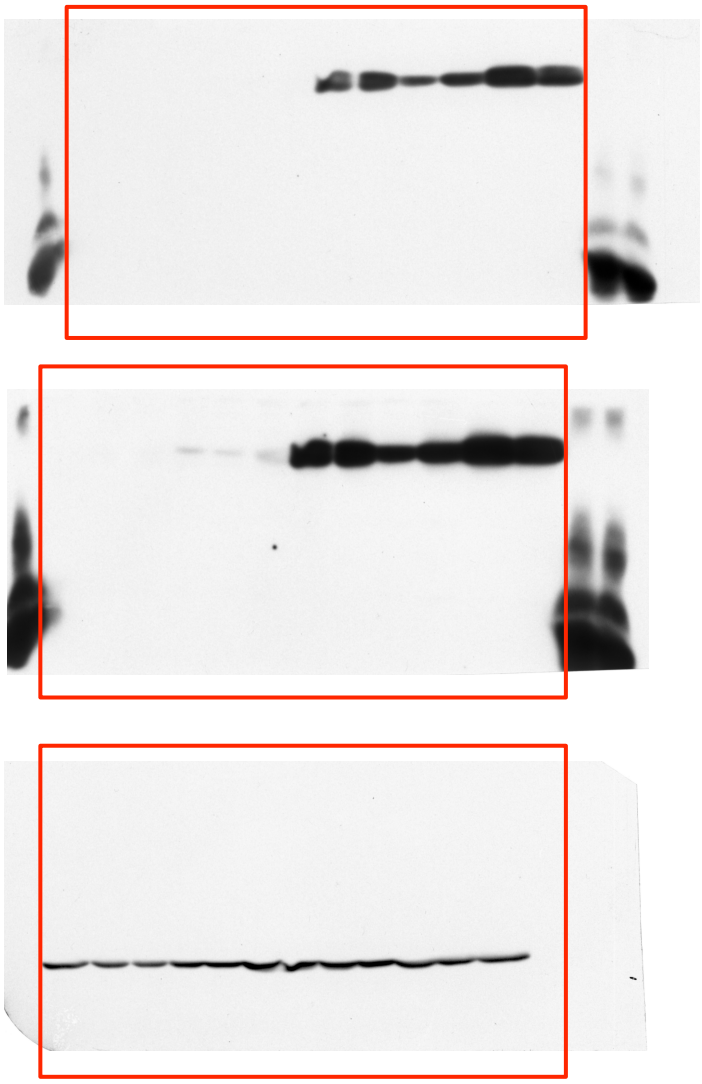

Figure S17. Full uncut gels of Figure 3C.

Table S1. Gap-length frequency analysis of the albumin on-target site (*sgRNA8*)

Table S1

Gap-length frequency analysis at the *albumin* on-target site (sgRNA8)

	Sample ID	Target sequence	N. of Reads	N. of gapped reads (≥2)	N. of gapped reads (≥1)	Percentage of reads with gaps≥2	Percentage of reads with gaps≥1	Maximum gap length	Mean gap length≥2	Mean gap length≥1	Median gap length≥2	Median gap length≥1
1	Mouse 4 (+)	*Albumin*	54986	10463	12543	**19.0**	**22.81**	306	**18.7**	**15.7**	**7**	**4**
2	Mouse 5 (+)	*Albumin*	16967	3115	3804	**18.4**	**22.42**	239	**10.4**	**8.7**	**5**	**4**
3	Mouse 6 (+)	*Albumin*	19176	2712	3419	**14.1**	**17.83**	237	**12.0**	**9.8**	**6**	**4**
4	Mouse (-)	*Albumin*	40676	78	809	**0.2**	**1.99**	69	**9.6**	**1.8**	**4**	**1**
5	Mouse 4 (+)	*Albumin*	137469	27215	32476	**19.8**	**23.62**	395	**13.7**	**11.7**	**7**	**4**
6	Mouse (-)	*Albumin*	41468	111	900	**0.3**	**2.17**	97	**20.6**	**3.4**	**5**	**1**

The genomic DNA of the albumin on-target site was PCR amplified and sequenced by NGS approach. The obtained reads were aligned and noise filtered. The % of reads containing gaps ≥ 2 bases was determined. Lines 5 and 6 show the data of independent duplicate PCR reactions of Lines 1 and 4. The animals are the ones presented in Figure 2C-D for *sgRNA8*. The length of the PCR fragment was 517 bp.

Table S2. Positional-frequency analysis of the albumin on-target site (*sgRNA8*)

Table S2

Positional-frequency analysis at the *albumin* on-target site (*sgRNA8*)

Sample ID	Variant	Filter	Min	Max	Mean	Median
Mouse 4 (+)	indel	Signal	1.4	15.1	4.7	**3.1**
Mouse 4 (+)	indel	Noise	0.0	1.4	0.7	**0.7**
Mouse 4 (+)	snp	Signal	ND	ND	ND	**ND**
Mouse 4 (+)	snp	Noise	0.0	1.4	0.2	**0.2**
Mouse 5 (+)	indel	Signal	1.7	14.7	5.4	**3.9**
Mouse 5 (+)	indel	Noise	0.0	1.6	0.2	**0.2**
Mouse 5 (+)	snp	Signal	ND	ND	ND	**ND**
Mouse 5 (+)	snp	Noise	0.0	1.5	0.3	**0.2**
Mouse 6 (+)	indel	Signal	1.6	11.1	4.7	**4.5**
Mouse 6 (+)	indel	Noise	0.0	1.5	0.2	**0.2**
Mouse 6 (+)	snp	Signal	ND	ND	ND	**ND**
Mouse 6 (+)	snp	Noise	0.0	1.4	0.2	**0.1**
Mouse (-)	indel	Noise	0.0	0.4	0.0	**0.0**
Mouse (-)	snp	Signal	ND	ND	ND	**ND**
Mouse (-)	snp	Noise	0.0	1.5	0.1	**0.1**

The genomic DNA of the albumin on-target site was PCR amplified and sequenced by NGS. The positional-frequency analysis of the obtained reads was performed as described in the Materials and Methods section. The animals are the ones presented in Figure 2C, D for *sgRNA8*. The median values were plotted in Figure S3C. ND, not detected.

Table S3. Positional-frequency analysis of predicted off-target sites

Table S3

Positional-frequency analysis of predicted off-target sites

			Kif21a				*Tubgcp2*			
Sample ID	Variant	Filter	Min	Max	Mean	**Median**	Min	Max	Mean	**Median**
Mouse 4 (+)	indel	Signal	ND	ND	ND	**ND**	ND	ND	ND	**ND**
Mouse 4 (+)	indel	Noise	0.001	0.168	0.019	**0.006**	0.003	0.244	0.024	**0.006**
Mouse 4 (+)	snp	Signal	1.450	1.678	1.564	**1.564**	ND	ND	ND	**ND**
Mouse 4 (+)	snp	Noise	0.014	0.948	0.149	**0.133**	0.011	1.234	0.177	**0.157**
Mouse 5 (+)	indel	Signal	ND	ND	ND	**ND**	ND	ND	ND	**ND**
Mouse 5 (+)	indel	Noise	0.002	0.246	0.026	**0.010**	0.006	0.234	0.042	**0.022**
Mouse 5 (+)	snp	Signal	1.508	2.309	1.741	**1.574**	1.718	1.808	1.763	**1.763**
Mouse 5 (+)	snp	Noise	0.014	1.324	0.194	**0.164**	0.009	1.419	0.274	**0.199**
Mouse 6 (+)	indel	Signal	ND	ND	ND	**ND**	ND	ND	ND	**ND**
Mouse 6 (+)	indel	Noise	0.001	0.179	0.018	**0.005**	0.002	0.224	0.021	**0.006**
Mouse 6 (+)	snp	Signal	1.657	1.804	1.730	**1.730**	ND	ND	ND	**ND**
Mouse 6 (+)	snp	Noise	0.015	0.957	0.136	**0.122**	0.017	1.228	0.163	**0.148**
Mouse (-)	indel	Noise	0.001	0.199	0.017	**0.004**	0.004	0.221	0.017	**0.013**
Mouse (-)	snp	Signal	1.489	1.945	1.717	**1.717**	ND	ND	ND	**ND**
Mouse (-)	snp	Noise	0.016	0.968	0.131	**0.116**	0.006	1.224	0.156	**0.135**

			Gm29874			
sample_id	sindel	pass	Min	Max	Mean	**Median**
Mouse 4 (+)	indel	Noise	0.001	0.477	0.019	**0.003**
Mouse 4 (+)	snp	Signal	1.624	2.637	2.000	**1.737**
Mouse 4 (+)	snp	Noise	0.023	1.368	0.208	**0.173**
Mouse 5 (+)	indel	Noise	0.001	0.408	0.030	**0.005**
Mouse 5 (+)	snp	Signal	1.528	2.540	1.889	**1.600**
Mouse 5 (+)	snp	Noise	0.012	1.319	0.205	**0.153**
Mouse 6 (+)	indel	Noise	0.001	0.528	0.027	**0.004**
Mouse 6 (+)	snp	Signal	1.648	2.592	1.900	**1.681**
Mouse 6 (+)	snp	Noise	0.012	1.311	0.174	**0.141**
Mouse (-)	indel	Noise	0.001	0.499	0.027	**0.005**
Mouse (-)	snp	Signal	1.761	2.739	2.103	**1.810**
Mouse (-)	snp	Noise	0.016	1.431	0.155	**0.120**

The genomic DNA of the predicted potential off-target sites was PCR amplified and sequenced by NGS. The positional-frequency analysis of the obtained reads was performed as described in the Mat&Meth section. The animals are the ones presented in Figure 2C-D for *sgRNA8*. The median values were plotted in Figure S12B. ND, not detected.

Table S4. Gap-length frequency analysis of predicted off-target sites

Table S4

Gap-length frequency analysis of predicted off-target sites

	Sample ID	Target sequence	N. of Reads	N. of gapped reads (≥2)	N. of gapped reads (≥1)	Percentage of reads with gaps≥2	Percentage of reads with gaps≥1	Maximum gap length	Mean gap length≥2	Mean gap length≥1	Median gap length≥2	Median gap length≥1
1	Mouse 4 (+)	*Kif21a*	69776	146	1070	**0.2**	**1.5**	367	105.0	15.2	**2**	**1**
2	Mouse 4 (+)	*Tubgcp2*	37900	99	728	**0.3**	**1.9**	414	56.3	8.5	**3**	**1**
3	Mouse 5 (+)	*Kif21a*	43506	78	696	**0.2**	**1.6**	368	82.1	10.1	**2**	**1**
4	Mouse 5 (+)	*Tubgcp2*	22151	74	480	**0.3**	**2.2**	164	17.1	3.5	**5**	**1**
5	Mouse 6 (+)	*Kif21a*	79425	88	1143	**0.1**	**1.4**	366	70.5	6.3	**2**	**1**
6	Mouse 6 (+)	*Tubgcp2*	48061	84	830	**0.2**	**1.7**	59	8.7	1.8	**3**	**1**
7	Mouse (-)	*Kif21a*	110129	192	1610	**0.2**	**1.5**	370	76.3	10.0	**2**	**1**
8	Mouse (-)	*Tubgcp2*	32617	67	580	**0.2**	**1.8**	230	14.1	2.5	**3**	**1**
9	Mouse 4 (+)	*Gm29874*	135024	1136	3671	**0.8**	**2.7**	385	201.9	63.2	**378**	**1**
10	Mouse 5 (+)	*Gm29874*	86507	410	1976	**0.5**	**2.3**	385	88.1	19.1	**4**	**1**
11	Mouse 6 (+)	*Gm29874*	109815	840	2814	**0.8**	**2.6**	386	168.3	50.9	**21**	**1**
12	Mouse (-)	*Gm29874*	171007	1186	4229	**0.7**	**2.5**	385	161.0	45.9	**4**	**1**

The genomic DNA of the predicted potential off-target sites was PCR amplified and sequenced by NGS. The obtained reads were aligned and noise filtered. The % of reads containing gaps ≥ 2 bases was determined. The animals are the ones presented in Figure 2C-D for *sgRNA8*. The length of the PCR fragments was *Tubgcp2*, 522 bp; *Kif21a*, 478 bp; and *Gm29874*, 491 bp.

Table S5. Description of animal treatments

Table S5

Description of animal treatments

Day of delivery (Post-natal day)	Mice	Route of administration	rAVV8 vectors	Dose (vg/mouse)	Objective	Figure
P4	*WT*	IP	rAAV8-SaCas9-sgRNA8 and rAAV8-SaCas9-sgRNA7	1.0E+12	*Sa*Cas9-sgRNA8 efficiency	Fig. 2C, D
P4	*WT*	IV	rAAV8-donor-eGFP	8.0E+11	HDR efficiency (low SaCas9 dose)	Fig. 3
			rAAV8-SaCas9-sgRNA8	2.0E+11		
			rAAV8-donor-eGFP	8.0E+11	HDR efficiency (high SaCas9 dose)	
			rAAV8-SaCas9-sgRNA8	6.0E+11		
P2	*Ugt1*$^{-/-}$	IV	rAAV-donor-hUGT1A1	2.0E+11	HDR efficiency (low SaCas9 dose)	Fig. 4
			rAAV8-SaCas9-sgRNA8	6.0E+10		
			rAAV-donor-hUGT1A1	2.0E+11	HDR efficiency (high SaCas9 dose)	
			rAAV8-SaCas9-sgRNA8	2.0E+11		
P4	*WT* (same mice of Fig. 2)	IP	rAAV8-SaCas9-sgRNA8 and rAAV8-SaCas9-sgRNA7	1.0E+12	*Sa*Cas9-sgRNA8 on-target efficiency	Supp. Fig. 3
P4	*WT*	IP	rAAV8-SaCas9-sgRNA8	2.5E+11	*Sa*Cas9-sgRNA8 dose-finding experiment	Supp. Fig. 4
				5.0E+11		
				7.5E+11		
				1.0E+12		
P4	*WT*	IP	pGG2-AAT-eGFP	1.0E+11	IP vs. IV comparison	Supp. Fig. 5
		IV				
P2	*WT*	IV	rAAV8-donor-eGFP	8.0E+11	P2 vs. P4 comparison	Supp. Fig. 6
P4						
P2	*WT*	IV	rAAV8-SaCas9-sgRNA8	2.0E+11	Determination of albumin mRNA at different time points after viral delivery	Supp. Fig. 10
P2	*WT* (same animals used in Supp. Fig. 10)	IV	rAAV8-SaCas9-sgRNA8	2.0E+11	Determination of SaCas9 at different time points after viral delivery	Supp. Fig. 11

Table S6. List of oligonucleotides coding for the sgRNAs

Table S6

List of oligonucleotides coding for the sgRNAs

Primer	5'-3' sequence	sgRNA encoded
sgRNA5_up	CACCGCATCCATCATTTCTTTGTTTT	*sgRNA5*
sgRNA5_down	AAACAAAACAAAGAAATGATGGATGC	
sgRNA6_up	CACCGACCCTGAAAACAAAGAAATG	*sgRNA6*
sgRNA6_down	AAACCATTTCTTTGTTTTCAGGGTC	
sgRNA7_up	CACCGAAAAGTATTAGCAGGACTGT	*sgRNA7*
sgRNA7_down	AAACACAGTCCTGCTAATACTTTTC	
sgRNA8_up	CACCGATGACCATACGTGAAGACCT	*sgRNA8*
sgRNA8_down	AAACAGGTCTTCACGTATGGTCATC	
sgRNA9_up	CACCGAGATGTCAGAGAGCCTGCTTT	*sgRNA9*
sgRNA9_down	AAACAAAGCAGGCTCTCTGACATCTC	

Table S7. Primers used to amplify the albumin target region

Table S7

Primers used to amplify the *albumin* target region

Primer	5'-3' sequence	Application	bp
FwStopmALB	GCCACACTGCTGCCTATTAAATACC	genomic PCR for T7E1 assay	787
RevStopmALB	CTTACATGAACCACTATGTGGAGTCC		

Table S8. List of oligonucleotides used for qRT-PCR

Table S8

List of oligonucleotides used for qRT-PCR

Primer	5'-3' sequence
GFP For	TGCCCGACAACCACTACCTG
Alb11R	TGAGTCCTGAGTCTTCATGTCTT
Alb10F	CTGACAAGGACACCTGCTTC
Alb11R	TGAGTCCTGAGTCTTCATGTCTT
mTNFa_DIR	TTCGAGTGACAAGCCTGTAG
mTNFa_REV	AGACAAGGTACAACCCATCG
mCD8aDIR	TCAGTTCTGTCGTGCCAGTC
mCD8_ex2_rev	GCACTGGCTTGGTAGTAGTA
mCD4DIR	GCAGCATGGCAAAGGTGTAT
mCD4REV	AAACGATCAAACTGCGAAGG
mIFNg For	CACGGCACAGTCATTGAAAG
mIFNg Rev	TTGCTGATGGCCTGATTGTC
mALB For	GCATGAAGTTGCCAGAAGAC
mALB Rev	TCTGCATACTGGAGCACTTC
RT-mGAPDH dir	ATGGTGAAGGTCGGTGTGAA
RT-mGAPDH rev	GTTGATGGCAACAATCTCCA

Table S9. List of antibodies

Table S9

Antibodies

Protein name	Supplier	#code	Source	Application	Dilution
eGFP	Santa Cruz	sc-8334	rabbit polyclonal	WB	1:1000
Actin	Sigma-Aldrich	A-2066	rabbit polyclonal	WB	1:2000
hUgt1a1	Santa Cruz	H-300	rabbit polyclonal	WB	1:600
SaCas9	abcam	EPR19795	rabbit monoclonal	WB	1:5000
Hsp70	Sigma-Aldrich	H-5147	rat polyclonal	WB	1:8000
hUgt1a1	Sigma-Aldrich	SAB2701158	rabbit polyclonal	IF	1:200
Calbindin	Synaptic Systems	214002	rabbit polyclonal	IF	1:400

Table S10. List of oligonucleotides used for NGS sequencing of on- and off-targets

Table S10

Oligonucleotides used for Illumina sequencing of on- and off-targets

Primer	5'-3' sequence
Gm29874_for2_tail	TCGTCGGCAGCGTCAGATGTGTATAAGAGACAGATCTTATGGACTGAGCCACC
Gm29874_rev2_tail	GTCTCGTGGGCTCGGAGATGTGTATAAGAGACAGTAGAGGTGGACTTCAGCATG
Kif21a_FOR1_tail	TCGTCGGCAGCGTCAGATGTGTATAAGAGACAGCAAGGACCTTTAGCCTCTGA
Kif21a_REV2_tail	GTCTCGTGGGCTCGGAGATGTGTATAAGAGACAGTGTCAGGCTACCAAGGATAC
Tubgcp2_FOR2_tail	TCGTCGGCAGCGTCAGATGTGTATAAGAGACAGAAGGCAGAGACCTTCAGTTG
Tubgcp2_REV2_tail	GTCTCGTGGGCTCGGAGATGTGTATAAGAGACAGTGGAGAAACACTTGAGGCAG
pAB1403dir_tail	TCGTCGGCAGCGTCAGATGTGTATAAGAGACAGGCCTATGGCTATGAAGTGCAAATCCTA
Revstop_malb_tail	GTCTCGTGGGCTCGGAGATGTGTATAAGAGACAGGGACTCCACATAGTGGTTCATGTAAG

In red are present the tails for Illumina seq as requested by BMR Genomics